Probabilistic Engineering Mechanics 34 (2013) 157–167

Contents lists available at ScienceDirect

Probabilistic Engineering Mechanics

journal homepage: www.elsevier.com/locate/probengmech

Karhunen–Loève expansion for multi-correlated stochastic processes

H. Cho, D. Venturi, G.E. Karniadakis *

Division of Applied Mathematics, Brown University, Providence, RI 02912, USA

ARTICLE INFO

Article history:
Received 10 December 2012
Received in revised form
4 September 2013
Accepted 19 September 2013
Available online 28 September 2013

Keywords:
Colored random noise
High-dimensional systems

ABSTRACT

We propose two different approaches generalizing the Karhunen–Loève series expansion to model and simulate multi-correlated non-stationary stochastic processes. The first approach (muKL) is based on the spectral analysis of a suitable assembled stochastic process and yields series expansions in terms of an identical set of uncorrelated random variables. The second approach (mcKL) relies on expansions in terms of correlated sets of random variables reflecting the cross-covariance structure of the processes. The effectiveness and the computational efficiency of both muKL and mcKL is demonstrated through numerical examples involving Gaussian processes with exponential and Gaussian covariances as well as fractional Brownian motion and Brownian bridge processes. In particular, we study accuracy and convergence rates of our series expansions and compare the results against other statistical techniques such as mixtures of probabilistic principal component analysis. We found that muKL and mcKL provide an effective representation of the multi-correlated process that can be readily employed in stochastic simulation and dimension reduction data-driven problems.

© 2013 Elsevier Ltd. All rights reserved.

1. Introduction

Stochastic simulation, sensitivity analysis and optimization of multi-physics and multi-scale problems of interest in engineering often involve non-stationary random processes with mutual correlations. The effective mathematical representation of such processes is the key element for the efficiency of any computational approach that aims at providing quantitative results. Over the years many different techniques have been developed for this purpose. A popular one employs series expansions in terms of random variables. The series can be constructed, e.g., by using orthogonal polynomials [1,2], spectral density methods [3–6], wavelets [7–9], Karhunen–Loève (KL) decompositions [10–16], bi-orthogonal techniques [17–19] or functional principal component analyses [20–23]. Many of these methods have been developed for a single process or ensembles of statistically independent processes, and their generalization to multi-correlated processes and fields is not straightforward. Nevertheless, many systems of interest to engineering involve multi-correlated processes, for instance, earthquake ground motions [24,25], fluid–structure interaction [26,27], acoustic propagation [28,3] and multi-scale modeling of materials [29]. Thus, it is of fundamental importance to develop appropriate mathematical frameworks to model and simulate multi-correlated random processes effectively. The spectral density method [4,5] has been already extended to multivariate non-stationary random processes, providing good results in capturing the power-spectral density and the cross-spectral density [24,30]. In addition, the numerical efficiency can be improved by using fast transforms such as FFT, DFT, and digital filters. However, the spectral density method is limited to weakly stationary random processes. Another technique that has been proposed to represent multi-correlated processes is the mixture of probabilistic principal component analysis (moPPCA) [31,32]. In this method, one looks for a representation of multiple random processes in terms of a linear combinations of independent random variables. The expansion is usually constructed by analyzing a large amount of data which is then classified into a prescribed number of partitions while obtaining the principal axes for each partition. If the relational structure between the data is considered only within each partition then we have the so-called probabilistic relational PCA [33]. A related approach has been recently introduced by Vořechovský [34].

In this paper, we propose two methods that extend the classical KL expansion to multi-correlated non-stationary stochastic processes. The first is based on the spectral decomposition of a suitable *assembled process* and yields series expansions in terms of an identical set of *uncorrelated* random variables. A similar strategy has been proposed in the context of functional principal component analysis [35]. The second approach relies on expansions in terms of *correlated* sets of random variables. The cross-covariance structure of the processes is imposed by setting the cross-correlation between such sets of random variables appropriately. Both these methods are straightforward to use and can be readily employed in stochastic simulations based

* Corresponding author. Tel.: +1 401 863 1217; fax: +1 401 863 2722.
E-mail address: george_karniadakis@brown.edu (G.E. Karniadakis).

0266-8920/$ - see front matter © 2013 Elsevier Ltd. All rights reserved.
http://dx.doi.org/10.1016/j.probengmech.2013.09.004

on Monte-Carlo, polynomial chaos [10,36] or probabilistic collocation [37].

This paper is organized as follows. In Section 2, we present the KL expansion for multi-correlated processes and introduce the multiple uncorrelated (muKL) and multiple correlated (mcKL) expansion methods. The effectiveness and the computational efficiently of both methods is discussed in Section 3. In Section 4 we present an application of muKL to a tumor growth model driven by two mutually correlated stochastic processes. Finally, the main findings and their implications are summarized in Section 5.

2. KL expansion for multi-correlated processes

Let us consider an ensemble of n zero-mean, square integrable random processes

$$\{f_1(t;\omega),\ldots,f_n(t;\omega)\} \tag{1}$$

in a complete probability space $(\Omega,\mathcal{F},P)$, where $\omega\in\Omega$, Ω denotes the sample space, $\mathcal{F}$ is a σ-field on Ω, and P is the applicable probability measure on $\mathcal{F}$. We assume that each process is defined in a bounded time interval $[0,T]$. The correlation structure between the processes $\{f_1(t;\omega),\ldots,f_n(t;\omega)\}$ can be represented in terms of $n(n+1)/2$ covariance kernels C_{ij},

$$C_{ij}(s,t)\overset{\text{def}}{=}\mathbb{E}[f_i(t;\omega)f_j(s;\omega)],\quad 1\le i\le j\le n,$$

where $\mathbb{E}[\cdot]$ denotes the statistical expectation operator. The quantity $C_{ii}(s,t)$ is the auto-covariance of the process $f_i(t;\omega)$, which will also be denoted as $C_i(s,t)$, for notational convenience. If the processes $\{f_1(t;\omega),\ldots,f_n(t;\omega)\}$ are mutually independent, then the classical KL expansion can be applied to each process, leading to multiple series which can be constructed separately [11,15]. However, if the cross-covariances $C_{ij}(s,t)$ are not zero, then it is not straightforward to obtain consistent expansions for all random processes, reflecting both the autocorrelation as well as the cross covariance structure.

Hereafter we propose two different methods to overcome this problem. The first relies on series expansions of all processes in terms of a single set of uncorrelated random variables (see also [35]). The second employs distinct but correlated sets of random variables for each process [30,34,38]. We will examine both stationary as well as non-stationary processes. In particular, we will consider Gaussian processes with exponential

$$C_i(s,t)=\frac{D_i}{\tau_i}\exp\left[-\frac{|t-s|}{\tau_i}\right] \tag{2}$$

and Gaussian

$$C_i(s,t)=\frac{D_i}{\tau_i}\exp\left[-6\frac{(t-s)^2}{\tau_i^2}\right] \tag{3}$$

covariances, where τ_i and D_i represent, respectively, the correlation length and the correlation amplitude of the process $f_i(t;\omega)$. We will also consider non-stationary covariances [39,40], such as those associated with fractional Brownian motion

$$C_i(s,t)=\frac{D_i}{2}(|s|^{2H_i}+|t|^{2H_i}-|s-t|^{2H_i}), \tag{4}$$

where $0<H_i<1$ is the Hurst parameter, and Brownian bridge

$$C_i(s,t)=D_i(\min(s,t)-st) \tag{5}$$

processes.

2.1. Multiple uncorrelated KL expansions (muKL)

In this method we look for a series expansion of each random process in (1) in terms of a single set of uncorrelated random variables. In order to construct such a series, we first consider an *assembled process* $\tilde f(t;\omega)$ defined as

$$\tilde f(t;\omega)\overset{\text{def}}{=}f_i(t-T_{i-1};\omega),\quad t\in\mathcal{I}_i, \tag{6}$$

where $T_i=iT$, $\mathcal{I}_1=[0,T_1]$ and $\mathcal{I}_i=(T_{i-1},T_i]$ $(1\le i\le n)$. In other words, the restriction of the assembled process $\tilde f(t;\omega)$ to the time interval $\mathcal{I}_i$ coincides with the process $f_i(t;\omega)$. Note that here we assumed that all processes in (1) are defined on the same time interval $[0,T]$, although this requirement can be easily relaxed. Obviously, $\tilde f(t;\omega)$ is still a second-order process satisfying

$$\mathbb{E}[\tilde f(t;\omega)]=0,\quad \mathbb{E}[\tilde f(t;\omega)\tilde f(s;\omega)]=\tilde C(s,t), \tag{7}$$

where the assembled covariance function $\tilde C(s,t)$ is defined as

$$\tilde C(s,t)\overset{\text{def}}{=}C_{ij}(s-T_{i-1},t-T_{j-1}),\quad s\in\mathcal{I}_i,\ \ t\in\mathcal{I}_j. \tag{8}$$

At this point, we look for a KL-type expansion of the assembled process (6) in the form

$$\tilde f(t;\omega)=\sum_{k=1}^{\infty}\sqrt{\lambda_k}\tilde f_k(t)\xi_k(\omega), \tag{9}$$

where $\xi_k(\omega)$ are *uncorrelated* random variables

$$\xi_k(\omega)\overset{\text{def}}{=}\frac{1}{\sqrt{\lambda_k}}\int_0^{T_n}\tilde f(t;\omega)\tilde f_k(t)\,dt, \tag{10}$$

while λ_k and $\tilde f_k(t)$ are, respectively, eigenvalues and eigenfunctions of a symmetric compact integral operator [41,42] with kernel (8), i.e., they are solutions to the homogeneous Fredholm integral equation of the second kind

$$\int_0^{T_n}\tilde C(s,t)\tilde f(s)\,ds=\lambda\tilde f(t). \tag{11}$$

However, our assembled covariance $\tilde C(s,t)$ could not be positive semi-definite, even when all the covariances are positive semi-definite. This might lead to negative eigenvalues. For practical applications it is desirable to have a non-negative operator. In a discrete setting this yields the following positivity condition for the assembled discretized covariance $\tilde C(t_i,t_j)$:

$$\sum_{j=1}^{m}\sum_{i=1}^{m}\tilde C(t_i,t_j)x_ix_j\ge 0, \tag{12}$$

for any finite time sequence $\{t_1,\ldots,t_m\}$ and real numbers $\{x_1,\ldots,x_m\}$. In other words, the $m\times m$ matrix

$$\tilde C=\begin{bmatrix}\tilde C(t_1,t_1) & \tilde C(t_1,t_2) & \cdots & \tilde C(t_1,t_m)\\ \tilde C(t_2,t_1) & \tilde C(t_2,t_2) & \cdots & \tilde C(t_2,t_m)\\ \vdots & \vdots & \ddots & \vdots\\ \tilde C(t_m,t_1) & \tilde C(t_m,t_2) & \cdots & \tilde C(t_m,t_m)\end{bmatrix} \tag{13}$$

should be positive semi-definite for any set of m distinct time instants in $[0,T]$. As we will see in Section 2.1.1, the positivity requirement introduces several constraints, e.g., in the cross-correlation lengths. Once we have the available eigen-pair $\{\lambda_k,\tilde f_k(t)\}$ $(k=1,2,\ldots)$, ordered according to the magnitude of the eigenvalues λ_k, then we represent each eigenfunction $\tilde f_k(t)$ in terms of n *sub-components* $\phi_k^{(i)}(t)$ $(i=1,\ldots,n)$ defined as

$$\phi_k^{(i)}(t)\overset{\text{def}}{=}\tilde f_k(t+T_{i-1})\mathcal{I}_{[0,T]}(t), \tag{14}$$

where $\mathcal{I}_{[0,T]}$ is the indicator function on the set $[0,T]$. In this way, the i-th random process $f_i(t;\omega)$ is expanded as

$$f_i(t;\omega)=\sum_{k=1}^{\infty}\sqrt{\lambda_k}\phi_k^{(i)}(t)\xi_k(\omega). \tag{15}$$

Note that λ_k and $\xi_k(\omega)$ appearing in this equation are the same as those appearing in the assembled process (9). For each specific index i, the set of sub-components $\{\phi_k^{(i)}(t)\}$ $(k=1,2,\ldots)$ is not orthogonal[1] nor normalized in $t\in[0,T]$. However, $\phi_k^{(i)}(t)$ can be easily normalized within the time interval $[0,T]$. This leads to the following series:

$$f_i(t;\omega)=\sum_{k=1}^{\infty}\sqrt{\hat{\lambda}_k^{(i)}}\,\hat{\phi}_k^{(i)}(t)\xi_k(\omega), \tag{16}$$

where $\hat{\phi}_k^{(i)}(t)\overset{\text{def}}{=}\phi_k^{(i)}(t)/\|\phi_k^{(i)}(t)\|_2$ and $\hat{\lambda}_k^{(i)}\overset{\text{def}}{=}\lambda_k\|\phi_k^{(i)}(t)\|_2^2$. We remark that each random process in (15) or (16) is represented in terms of the same set of random variables ξ_i. Therefore, the muKL method cannot be used to represent heterogeneous sets of processes, i.e., processes with different types of random variables in the series expansion.

Next, we study the convergence properties of truncated muKL expansions. To this end, let us first define the truncated assembled process as

$$S_M(t;\omega)\overset{\text{def}}{=}\sum_{k=1}^{M}\sqrt{\lambda_k}\tilde{f}_k(t)\xi_k(\omega), \tag{17}$$

and the corresponding mean-squared error as

$$\varepsilon_M^2\overset{\text{def}}{=}\int_0^{T_n}\mathbb{E}[(\tilde{f}(t;\omega)-S_M(t;\omega))^2]\,dt. \tag{18}$$

By using the fact that ξ_k are uncorrelated and that $\tilde{f}_k$ are orthonormal, we immediately obtain

$$\varepsilon_M^2=\sum_{k=M+1}^{\infty}\lambda_k, \tag{19}$$

i.e., the truncation error of the series (9) decreases with respect to the decay rate of the eigenvalues. The quantity ε_M^2 also provides an upper bound for the truncation error of the muKL expansion (15). In fact, we have

$$\int_0^T\mathbb{E}\left[\left(f_i(t)-\sum_{k=1}^{M}\sqrt{\lambda_k}\phi_k^{(i)}(t)\xi_k\right)^2\right]dt = \int_{T_{i-1}}^{T_i}\mathbb{E}[(\tilde{f}(t)-S_M(t;\omega))^2]\,dt\le\varepsilon_M^2. \tag{20}$$

In addition, the errors of the cross-covariances C_{ij} are bounded by the error of the assembled covariance $\tilde{C}(t,s)$ in Eq. (8). In fact, by Mercer's theorem [42], the quantity

$$\varepsilon_M^{\tilde{C}}\overset{\text{def}}{=}\frac{1}{\|\tilde{C}(s,t)\|_1}\int_0^{T_n}\int_0^{T_n}\left|\tilde{C}(s,t)-\sum_{k=1}^{M}\lambda_k\tilde{f}_k(s)\tilde{f}_k(t)\right|dt\,ds \tag{21}$$

goes to zero uniformly in M, and this implies that

$$\frac{1}{\|\tilde{C}(s,t)\|_1}\int_0^T\int_0^T\left|C_{ij}(s,t)-\sum_{k=1}^{M}\lambda_k\phi_k^{(i)}(s)\phi_k^{(j)}(t)\right|dt\,ds \tag{22}$$

is bounded by $\varepsilon_M^{\tilde{C}}$. Similar results hold for the covariances $C_i(s,t)$. The proper choice of M in (17) can be done, e.g., by imposing a certain threshold for the errors ε_M or $\varepsilon_M^{\tilde{C}}$. Based on Eq. (19), this is equivalent to set a threshold for the relative cumulative spectrum, e.g.,

$$\sum_{k=1}^{M}\lambda_k\ge 0.95\sum_{k=1}^{\infty}\lambda_k. \tag{23}$$

[1] The spectral theorem [41] guarantees that the solutions to Eq. (11) are orthonormal in $L_2([0,T_n])$. This does not obviously imply that their sub-components are orthogonal as well.

2.1.1. Positivity constraints for exponential covariances

We have seen in the previous section that the assembled covariance kernel (8) is, in general, not positive semi-definite. This could yield negative eigenvalues in the expansion of the assembled process and, consequently, in the expansions of all processes. In practical applications it is convenient to have positive eigenvalues. This requirement induces a positivity constraint in the integral operator at the left hand side of (11). In order to understand the implications of such a constraint, let us consider a simple prototype problem involving two random processes, $f_1(t;\omega)$ and $f_2(t;\omega)$, with exponential covariances and cross-covariance as in Eq. (2). We choose two time instants $(s_1,s_2)\in[0,T]^2$, such that $t_1=s_1$ and $t_2=s_2+T$. This yields the following assembled covariance kernel:

$$\tilde{C}=\begin{bmatrix}\frac{1}{\tau_1} & \frac{1}{\tau_{12}}\exp\left[-\frac{|s_1-s_2|}{\tau_{12}}\right]\\ \frac{1}{\tau_{12}}\exp\left[-\frac{|s_1-s_2|}{\tau_{12}}\right] & \frac{1}{\tau_2}\end{bmatrix},$$

which must be positive semi-definite for all s_1 and s_2. An equivalent statement for a matrix to be positive semi-definite is that all the eigenvalues are non-negative and a necessary condition is that the determinant is non-negative. In our case, this yields

$$\det[\tilde{C}]=\frac{1}{\tau_1\tau_2}-\frac{1}{\tau_{12}^2}\exp\left[-2\frac{|s_1-s_2|}{\tau_{12}}\right]\ge 0, \tag{24}$$

which is verified for all s_1 and s_2 provided $\tau_1\tau_2\le\tau_{12}^2$. This result can be extended to n exponentially correlated random processes by choosing $t_1\in[T_{i-1},T_i]$ and $t_2\in[T_{j-1},T_j]$, where $i<j$. By using similar arguments we obtain that the assembled covariance kernel is non-negative if the correlation lengths satisfy

$$\tau_i\tau_j\le\tau_{ij}^2. \tag{25}$$

This positivity condition holds also for processes with Gaussian covariances in the form (3). In summary, the set of correlation lengths $\{\tau_{ij}\}$ for which the muKL method is applicable is *bounded*. The exact range will be determined numerically in Section 3. Constraints of type Eq. (25) arise as a consequence of the assumption that each process f_i is a linear combination of an identical set of random variables. In order to see this, let us revisit the example above and assume that each process has the same correlation length, i.e., $\tau_i=\tau_j$. In this case the positivity condition of the assembled covariance is satisfied by the requirement $\tau_i=\tau_j\le\tau_{ij}$. Thus, the cross-correlation length between two processes must be larger than the correlation length of each process. In other words, expanding different random processes relatively to the same set of random variables (as done in muKL) makes sense if the processes are "enough correlated" to each other.

2.2. Multiple correlated KL expansion (mcKL)

Differently from the muKL technique introduced so far, where only one set of uncorrelated random variables was used to represent the whole set of stochastic processes (1), the mcKL expansion method employs different sets of mutually correlated random variables. Let

$$f_i(t;\omega)=\sum_{k=1}^{\infty}\sqrt{\gamma_k^i}\psi_k^i(t)\eta_k^i(\omega) \tag{26}$$

be the standard KL expansion of $f_i(t;\omega)$. For a fixed index i, $\{\gamma_k^i,\psi_k^i(t)\}$ are eigen-pairs of the auto-covariance $C_i(s,t)$, while $\{\eta_k^i(\omega)\}$ is a set of zero-mean uncorrelated random variables with unit variance. Upon definition of

$$K_{km}^{ij}\overset{\text{def}}{=}\mathbb{E}[\eta_k^i\eta_m^j], \tag{27}$$

we obtain from Eq. (26) the cross-covariances

$$C_{ij}(s,t) = \mathbb{E}[f_i(s;\omega)f_j(t;\omega)] = \sum_{k,m=1}^{\infty} K_{km}^{ij}\sqrt{\gamma_k^i\gamma_m^j}\psi_k^i(s)\psi_m^j(t). \quad (28)$$

The correlation constants K_{km}^{ij} in Eq. (27) can be determined by projecting the kernels $C_{ij}(s,t)$ onto the eigenfunction set of each random process. This yields (see also [1])

$$K_{km}^{ij} = \frac{1}{\sqrt{\gamma_k^i\gamma_m^j}}\int_0^T\int_0^T C_{ij}(s,t)\psi_k^i(s)\psi_m^j(t)\,ds\,dt. \quad (29)$$

Let K be the block matrix

$$K \overset{\text{def}}{=} \begin{bmatrix} I & K^{12} & \cdots & K^{1n} \\ K^{21} & I & \cdots & K^{2n} \\ \vdots & \vdots & \ddots & \vdots \\ K^{n1} & K^{n2} & \cdots & I \end{bmatrix}, \quad (30)$$

where I is the identity matrix and K^{ij} is the matrix defined in Eq. (29). Note that, in general, K is symmetric but not necessarily positive definite. We will revisit this issue in Section 3.2.

The next question is how to obtain the random variables $\{\eta_k^i(\omega)\}$ in Eq. (26) from K_{km}^{ij}. To this end, let

$$\eta \overset{\text{def}}{=} \begin{bmatrix} \{\eta_k^1(\omega)\} \\ \{\eta_k^2(\omega)\} \\ \vdots \\ \{\eta_k^n(\omega)\} \end{bmatrix} \quad (31)$$

be a correlated random vector collecting all random variables $\{\eta_k^i(\omega)\}$ in which the processes (26) are expanded. In order to generate realizations η we assume that K is positive definite and perform a Cholesky decomposition in the form $K = RR^T$. Then we transform the random variables as $\tilde{\eta} = R^{-1}\eta$. This yields $\mathbb{E}[\tilde{\eta}\tilde{\eta}^T] = I$, i.e., the random vector $\tilde{\eta}$ has uncorrelated components. Thus, in order to represent our processes we can first consider a set of uncorrelated random variables $\tilde{\eta}$ and then transform them into the specified correlated set η by simply applying R to $\tilde{\eta}$.[2] The eigenfunctions $\psi_k^i(t)$ in (26) can be transformed as well by applying R to the right. In fact, if we denote by $\Psi(t)$ the vector collecting the eigenfunctions of all the auto-covariances, then we have $\tilde{\Psi}(t) = \Psi(t)R$.

The series expansions (26) obtained in this way satisfy the correlation structure (28). Similar expansions have been obtained by Vořechovský [34], by directly imposing the correlation constants rather than considering their expression in terms of cross-covariance kernels. The truncation error of the mcKL series can be defined as the summation of the error in each covariance kernel

$$\varepsilon_{M_{ij}}^{C_{ij}} \overset{\text{def}}{=} \frac{1}{\|C_{ij}(s,t)\|_1}\int_0^T\int_0^T |C_{ij}(s,t) - \sum_{k=1}^{M_i}\sum_{m=1}^{M_j} K_{km}^{ij}\cdot\sqrt{\gamma_k^i\gamma_m^j}\psi_k^i(s)\psi_m^j(t)|\,ds\,dt. \quad (32)$$

2.2.1. Analytical results for exponentially correlated processes

The eigenvalues and eigenfunctions of integral operators in the form (11) with exponential covariances (2) admit an analytical expression [10,44]. In particular, let $c_i = 1/\tau_i$, where τ_i is the correlation length of the process $f_i(t;\omega)$. Then γ_k^i and $\psi_k^i(t)$ in Eq. (26) are given by

$$\gamma_k^i = \frac{2c_i}{w_{ik}^2 + c_i^2} \quad (33)$$

$$\psi_k^i(t) = \frac{1}{A_{ik}}\left(\frac{w_{ik}}{c_i}\cos(w_{ik}t) + \sin(w_{ik}t)\right), \quad (34)$$

where w_{ik} $(k = 1, 2, \ldots)$ are solutions to the transcendental equation $(w_{ik}^2 - c_i^2)\tan(w_{ik}T) - 2c_i w_{ik} = 0$ and

$$A_{ik} = \left[\frac{1}{2}\left(1 + \frac{w_{ik}^2}{c_i^2}\right)T + \left(\frac{w_{ik}^2}{c_i^2} - 1\right)\frac{\sin(2w_{ik}T)}{4w_{ik}} + \frac{1}{2c_i}(1 - \cos(2w_{ik}T))\right]^{1/2}.$$

A substitution of Eqs. (33) and (34) into Eq. (29) yields the following analytical expression for the cross-covariances:

$$K_{km}^{ij} = B_{km}^{ij0}[B_{km}^{ij1} + B_{km}^{ij2}\cos(w_{ik}T) + B_{km}^{ij3}\sin(w_{ik}T)] \times [B_{km}^{ij4} + B_{km}^{ij5}\cos(w_{jm}T) + B_{km}^{ij6}\sin(w_{jm}T)],$$

where

$$B_{km}^{ij0} = \frac{c_{ij}^2 e^{-T/c_{ij}}}{A_{ik}A_{jm}c_i c_j(1 + c_{ij}^2 w_{ik}^2)(1 + c_{ij}^2 w_{jm}^2)}, \quad c_{ij} = \frac{1}{\tau_{ij}},$$
$$B_{km}^{ij1} = (1 + c_i c_{ij})e^{T/c_{ij}}w_{ik}, \quad B_{km}^{ij2} = -(1 + c_i c_{ij})w_{ik},$$
$$B_{km}^{ij3} = -c_i + c_{ij}w_{ik}^2, \quad B_{km}^{ij4} = (-1 + c_j c_{ij})w_{jm},$$
$$B_{km}^{ij5} = (1 - c_j c_{ij})e^{T/c_{ij}}w_{jm}, \quad B_{km}^{ij6} = (c_j + c_{ij}w_{jm}^2)e^{T/c_{ij}}.$$

Similar analytical results can be obtained for regularized exponential covariances [45]. Clearly, the availability of analytical results for the KL decomposition of each process f_i significantly reduces the computational cost of the mcKL method.

3. Numerical results

In this section we compare the proposed methods, i.e., muKL and mcKL (see Table 1), in terms of accuracy and computational cost. To this end, we consider multi-correlated random processes with both stationary and non-stationary covariances (2)–(5) in the time interval $[0, 1]$. Unless otherwise stated, we set $D_i = 1$, for all i. We first consider two exponentially correlated processes, $f_1(t;\omega)$ and $f_2(t;\omega)$. Several realizations (sample paths) of these processes are shown in Fig. 1 for $\tau_1 = 0.2$, $\tau_2 = 1$ and different cross-correlation lengths and amplitudes D_{12}. The truncation dimension in the muKL and mcKL series expansions (see Eqs. (22)–(32)) is set to $M = 50$ and $M_1 = M_2 = 25$, respectively. It is seen that, as we increase the cross-correlation length and amplitude the samples of f_1 and f_2 are more and more correlated, i.e., they tend to follow the same trend.

Imposing a cross-covariance between f_1 and f_2 results in different effects in muKL and mcKL expansions. In particular, in the muKL framework the cross covariance structure affects the basis functions $\phi_k^{(i)}$ in Eq. (14). On the other hand, in the mcKL framework the cross-covariance affects the correlation coefficients (29). Specifically, if the cross-correlation length is non-zero we see that several cross-correlation coefficients are activated (see Fig. 2).

Next, we compare muKL and mcKL methods in terms of accuracy. To this end we consider two correlated random processes with Gaussian covariances and cross-covariance. First of all, we examine the L_2 errors (21) and (32) as a function of the number of expansion terms M, and verify convergence of both muKL and mcKL expansions. This is done in Fig. 3 where we show the error of the assembled covariance kernel for different values of τ_1, fixed $\tau_2 = \tau_{12} = 2$, and $M_1 = M_2 = M/2$. It is seen that the error depends

[2] We recall that correlated non-normal random variables can also be transformed into a set of uncorrelated normal random variables by using Nataf transformation [43]. This technique first transforms each non-normal random variable into a normal random variable by using the inverse cumulative distribution function, and then apply the Cholesky decomposition to the correlation matrix to convert them into uncorrelated variables.

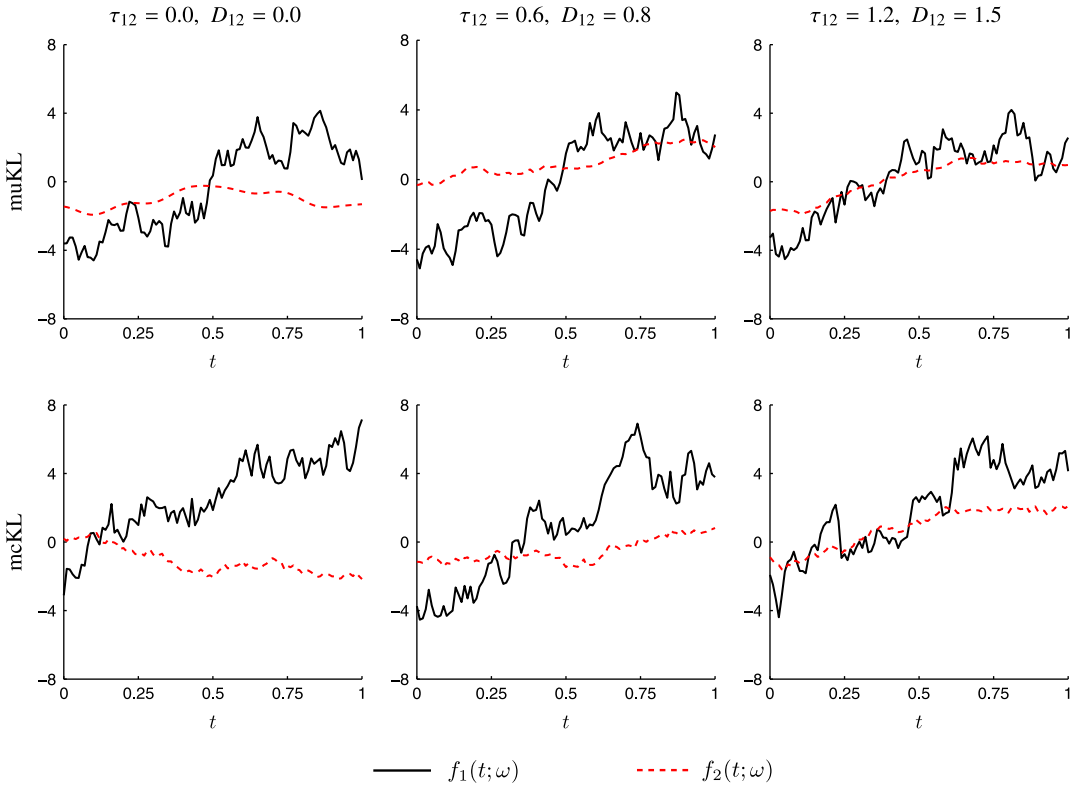

Fig. 1. Sample paths of two exponentially correlated random processes $f_1(t;\omega)$ and $f_2(t;\omega)$ generated by using muKL (first row) and mcKL (second row). Shown are results for $D_1 = D_2 = 1$, $\tau_1 = 0.2$, $\tau_2 = 1$ and different cross-covariance lengths τ_{12} and amplitudes D_{12}. It is seen that the sample paths of $f_2(t;\omega)$ tend to follow those of $f_1(t;\omega)$ when τ_{12} and D_{12} increase.

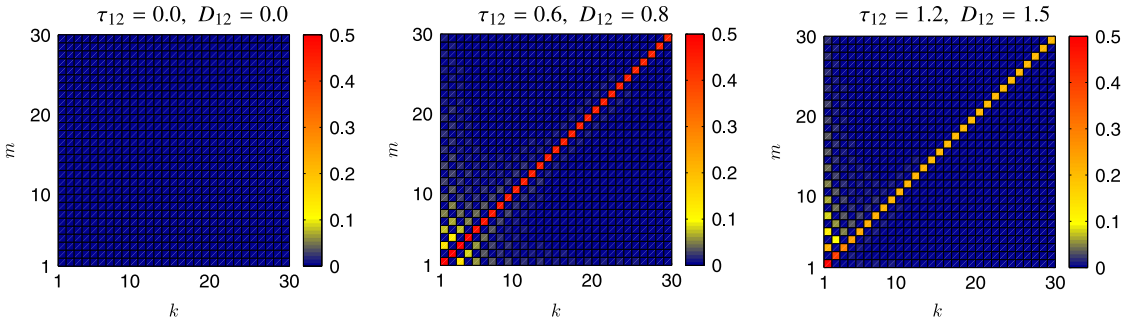

Fig. 2. Absolute value of the cross correlation coefficients K^{12}_{km} defined in Eq. (29). We see that for non-zero cross-correlation lengths τ_{12} several coefficients are activated.

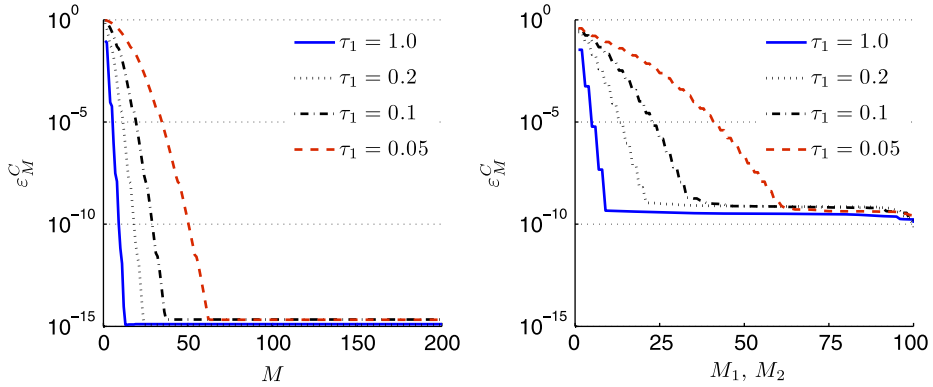

Fig. 3. L_2 error in the assembled Gaussian covariance $\tilde{C}$ by using muKL (left) and mcKL (right) expansions. Shown are results for different correlation lengths τ_1 and fixed $\tau_2 = \tau_{12} = 2$. Smaller correlation lengths require more random variables for a prescribed level of accuracy in both methods. However, muKL shows faster convergence and smaller errors than mcKL.

significantly on τ_1. In particular, the convergence of the series becomes slower as τ_1 decreases. Despite the smaller error in the first few dimensions of mcKL expansion, the convergence rate of the muKL expansion is faster than the mcKL expansion and the overall error is lower as well. The plateau observed in error plot of the mcKL method for large M is due to the correlation coefficients K_{ij}^{12}, which remain of order 10^{-10} for large k.

In Table 2 we summarize the number of random variables in muKL and mcKL expansions that yield 97% of the total energy of the processes, i.e., M is the truncation dimension defined by the condition $\varepsilon_M^{\tilde{C}} < 0.03$. As expected, muKL achieves the same level of accuracy by using less random variables than mcKL (see also Fig. 3). This is particularly true for *weakly correlated* processes, i.e. processes with small correlation length.

Next, we examine the error of exponentially correlated processes. This is done in Fig. 4, for the case $\tau_1 = 1$, $\tau_2 = 0.1$, $\tau_{12} = 1$. Note that the error decays slower compared to the Gaussian case. This is due to the fact that the exponential kernel is less smooth than the Gaussian one [46]. Fig. 4 also emphasizes different aspects in the decay of the covariance errors obtained by muKL and mcKL. In fact, the error in the cross covariance $\varepsilon_M^{C_{12}}$ decreases monotonically in mcKL, but not in muKL. Nevertheless, the total error turns out to be smaller by using muKL.

We also apply muKL and mcKL methods to random processes with non-stationary covariance functions. In particular, we consider fractional Brownian motion (FBM) and Brownian bridge (BB) processes (see Eqs. (4) and (5)). In Fig. 5 we show the *assembled covariances* for the specific cases we consider here, i.e., FBM and FBM/BB. The truncation dimensions for muKL and mcKL expansions are set to $M=48$ and $M_1 = 36$, $M_2 = 12$ in FBM, and to $M=54$ and $M_1 = 34$, $M_2 = 20$ in FBM/BB. With these parameters the absolute error in the representation of the covariances is less than 10^{-2} (see Fig. 6). Note that in both muKL and mcKL methods, the maximum error occurs at the locations where the covariance function is less smooth. In particular, the mcKL expansion exhibits larger absolute and L_2 errors in the cross-covariance function, which is consistent with previous results.

3.1. Computational cost

The muKL method requires solving an eigenproblem of size nN, where N denotes the number instants discretizing the time interval $[0, T]$. Thus, the computational cost of muKL is $O(n^3N^3)$. On the other hand, the mcKL expansion involves n eigendecompositions of size N, i.e., $O(nN^3)$. In addition, the projection of the eigenfunctions has to be computed. The computational cost of this operation is affected by the truncation dimensions M_1 and M_2 of the expansions and n, i.e., we obtain $O(M_iM_jn^2N^2)$. In Fig. 7 we compare the computation time (in s) required by muKL and mcKL to decompose n Gaussian correlated random processes with $\tau_i = 0.2$ and $\tau_{ij} = 1.0$. The expansions are truncated at $M=18n$ (muKL) and $M_i=18$ $(i = 1, \ldots, n)$ (mcKL).

Table 1
Summary of the algorithms for muKL and mcKL expansions.

muKL	mcKL
1. Assemble the random processes $\{f_1, \ldots, f_n\}$ and the covariance function as in Eqs. (6)–(8)	1. Apply KL expansion to each process as in Eq. (26)
2. Apply KL expansion to the assembled process (9)	2. Compute the correlation coefficients that yield the proper correlation structure (29)
3. Determine the basis function of each process and represent it as in Eqs. (14) and (15)	3. Represent each process as in (26), where η_j^k are determined by a singular value decomposition of (30)

Table 2
Number of random variables to achieve a truncation error smaller than 3%. The correlation lengths of the processes f_1 and f_2 are set as $\tau_1 = \tau$, $\tau_2 = 2\tau$, $\tau_{12} = 2\tau$. We see that the muKL expansion requires less random variables than the mcKL expansion, in particular for small τ.

τ	1.0	0.2	0.1	0.05	0.02
M (muKL)	2	5	7	13	31
(M_1, M_2) (mcKL)	(2, 1)	(3, 2)	(6, 3)	(11, 6)	(25, 13)

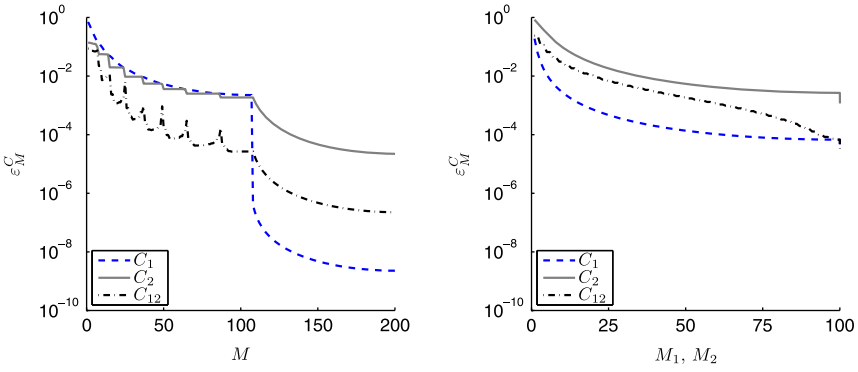

Fig. 4. L_2 errors in representing exponential covariances C_1, C_2, and C_{12} by using muKL (left) and mcKL (right). Here we set $\tau_1 = 1$, $\tau_2 = 0.1$, $\tau_{12} = 1$. Note that the error of C_{12} decreases monotonically in mcKL but not in muKL. The overall error is lower in muKL expansion.

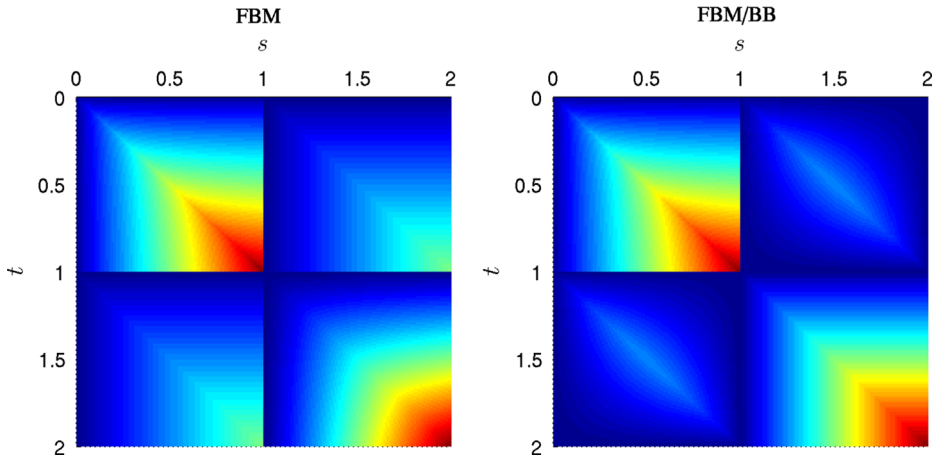

Fig. 5. Left: Assembled covariance function of two fractional Brownian motion (FBM) processes with Hurst indices $H_1=0.4$ and $H_2=0.7$. The cross covariance is also of FBM-type with $H_{12}=0.5$. Right: Assembled covariance of two FBM processes ($H_1=0.4$, $H_2=0.5$) with Brownian bridge (BB) cross-covariance. In both cases the correlation amplitudes are set to $D_1=1$, $D_2=1$ and $D_{12}=0.5$.

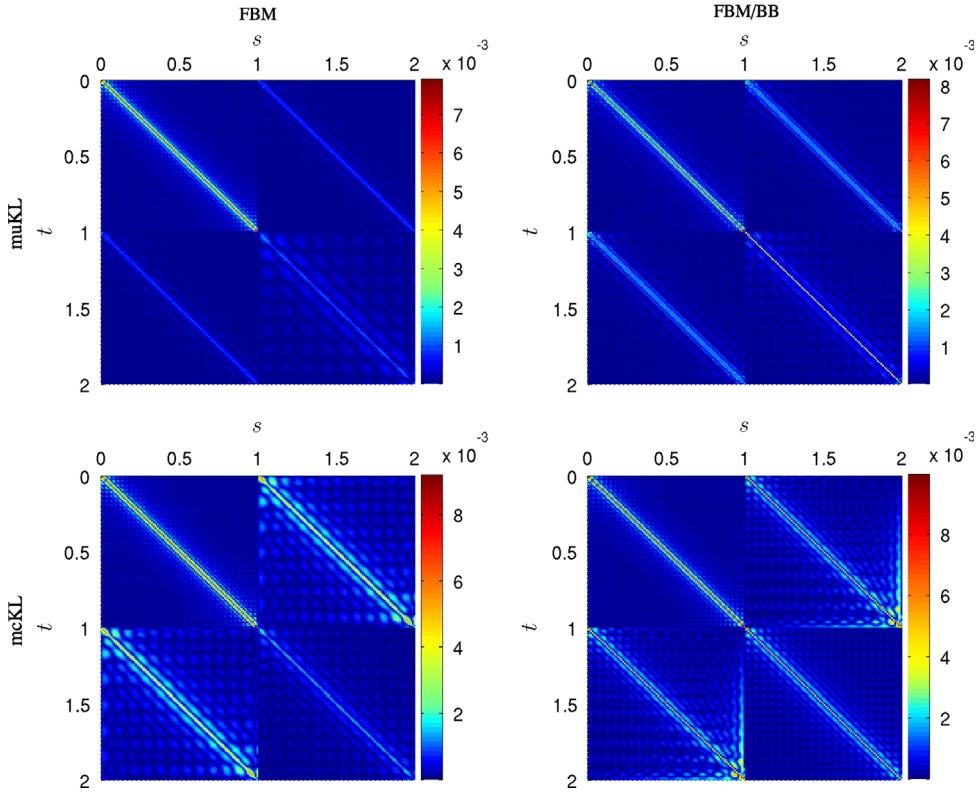

Fig. 6. Absolute errors of muKL (first row) mcKL (second row) in representing the assembled covariance functions shown in Fig. 5.

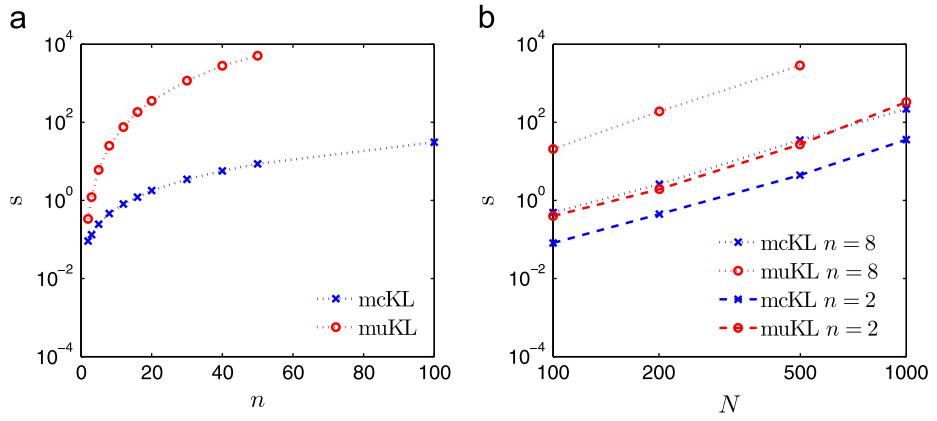

Fig. 7. (a) Computation time (in s) versus the number of random processes n; (b) computation time (in s) versus the number of degrees of freedom N in time domain (number of equally spaced points within $[0,1]$). The mcKL expansion is scalable and it requires less operations than the muKL.

3.2. Constraints for positive-definiteness

Both muKL and mcKL have to satisfy a positive-definiteness constraint. In fact, the assembled covariance function (8) in muKL and the correlation matrix (30) of the random variables in mcKL have to be positive-definite. In Fig. 8 we show the eigenvalues λ_k of the assembled exponential covariance kernel (13) and the minimum eigenvalue for different choices of the cross-correlation length τ_{12} and fixed $\tau_1 = \tau_2 = 0.1$. The existence of negative eigenvalues clearly indicates that the assembled covariance function is not always positive-definite. The minimum eigenvalue becomes negative when the cross-correlation length is small compared to the auto-correlation lengths of both processes. In the present example, this happens when $\tau_{12} \leq 0.1$, which coincides exactly with the theoretical condition we obtained in Eq. (25).

In Fig. 9, we plot the set of correlation lengths τ_2 and τ_{12} satisfying the positive-definiteness condition for exponential and Gaussian covariance kernels with $\tau_1 = 1$. Note that the analytical condition we obtained in Eq. (25) is in agreement with the numerical results and it provides a lower bound for τ_{12}, given τ_2. We also study the positive-definiteness constraint for *three* random processes. This is done in Fig. 10 where we plot the level sets of the cross-correlation lengths τ_{13} and τ_{23} for which the

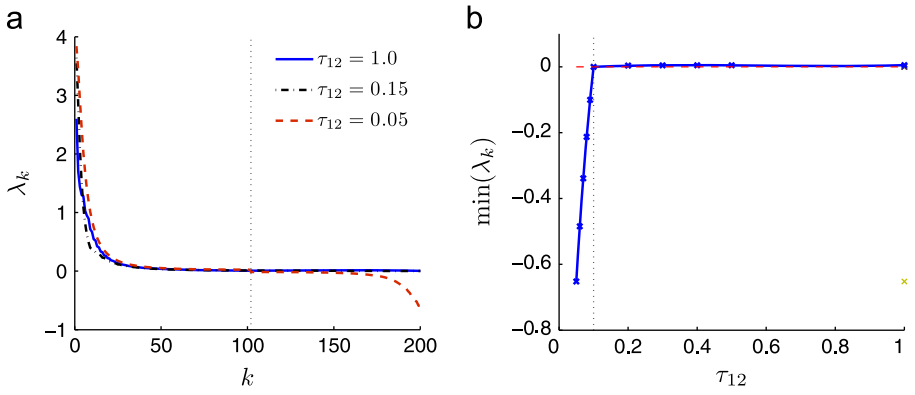

Fig. 8. (a) Eigenvalues λ_k of the assembled covariance kernel in muKL. (b) Smallest eigenvalue as a function of the cross-correlation lengths τ_{12}. Here we set $\tau_1 = \tau_2 = 0.1$. Note that all eigenvalues are positive for $\tau_{12} \geq 0.1$.

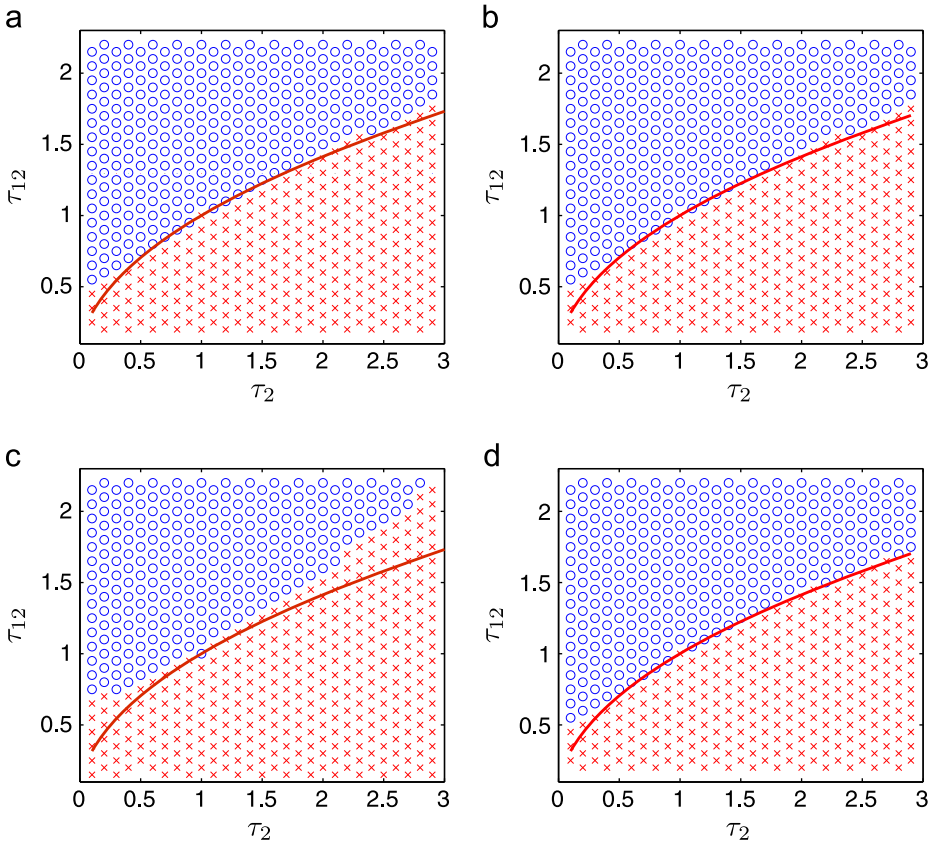

Fig. 9. Set of correlation lengths τ_2 and τ_{12} satisfying the positive-definiteness condition (circles) for $\tau_1 = 1$. We consider exponential covariance kernels in (a) and (b) and Gaussian covariance kernels in (c) and (d). In (a) and (c) we employ muKL while in (b) and (d) mcKL. The line denotes the theoretical constraint in Eq. (25) of the muKL expansion. We notice that not only muKL, but also mcKL satisfies a similar constraint.

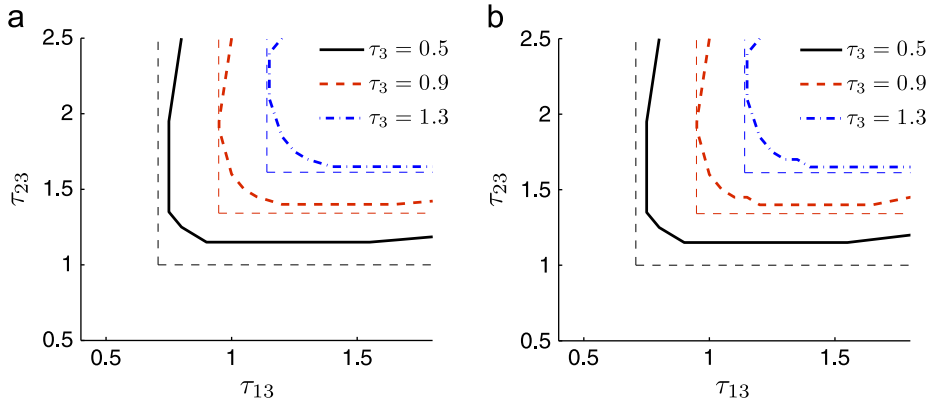

Fig. 10. Three Gaussian random processes. Level sets of the cross-correlation lengths τ_{13} and τ_{23} for which the minimum eigenvalue of the assembled covariance is zero. In particular, we set $\tau_1 = 1$, $\tau_2 = 2$ and $\tau_{12} = 5$ and consider different τ_3. Shown are results of muKL (a) and mcKL (b). The thin dashed lines are the analytical constraints in Eq. (25).

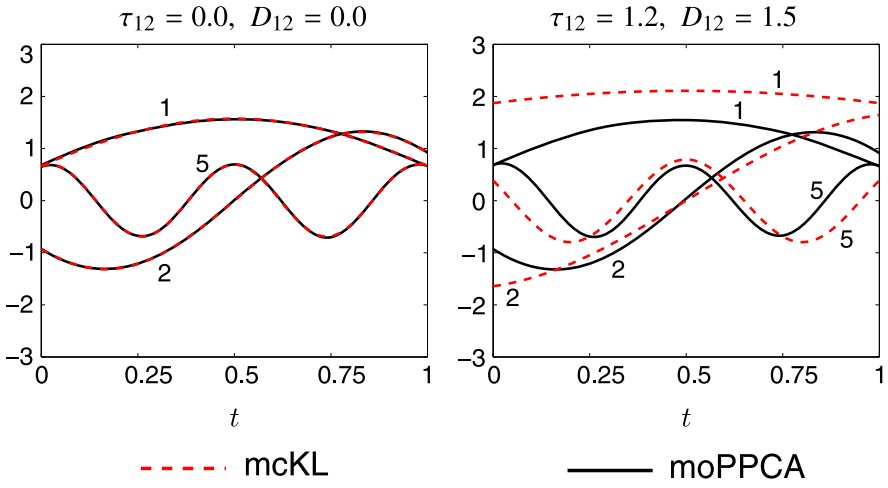

Fig. 11. Basis functions $\psi_1^1(t)$, $\psi_2^1(t)$ and $\psi_5^1(t)$ (denoted as 1, 2 and 5 for notational convenience) as computed by mcKL and moPPCA. Note the results of two methods coincide when f_1 and f_2 are uncorrelated ($\tau_{12} = 0$). Also, the eigenfunctions computed by moPPCA are insensitive to changes in τ_{12}. This suggests that moPPCA cannot represent cross-correlated random processes.

minimum eigenvalue of the assembled correlation is negative. Specifically we set $\tau_1 = 1$, $\tau_2 = 2$ and $\tau_{12} = 5$ and consider different values of τ_3. It is seen that the conditions in Eq. (25) still represent lower bounds for the cross-correlation lengths.

3.3. Comparison with moPPCA

In the multiple version of the probabilistic principal component analysis (moPPCA) [32] we look for a representation of multiple random processes in terms of a linear combinations of random variables. Therefore this method shares similar characteristics with the proposed mcKL. However, differently from mcKL, moPPCA assumes that all the random variables representing the processes are independent, while mcKL expansion drops such an assumption to impose cross-correlation. Therefore we expect that moPPCA cannot properly represent cross-correlated processes. In order to show this we consider two exponentially correlated random processes $f_1(t;\omega)$ and $f_2(t;\omega)$ having correlation lengths $\tau_1 = 0.2$, $\tau_2 = 1.0$, and τ_{12} equal to 0 and 1.2 as in Fig. 1. In Fig. 11 we compare the basis functions of $f_1(t;\omega)$ as computed by mcKL and moPPCA. Note that the results of the two methods coincide when f_1 and f_2 are uncorrelated ($\tau_{12} = 0$). Also, the eigenfunctions computed by moPPCA are insensitive to changes in τ_{12}. This suggests that moPPCA cannot represent cross-correlated random processes.

4. Application to a tumor cell growth model

Many recent studies aim at developing simple models of complex systems based on empirical or historical data [21,22,47]. This is the case, for example, of biological models described in terms of stochastic differential [48,49]. The muKL and mcKL methods can be applied in these contexts to find an appropriate representation of the random input processes, provided we have available their correlation structure, e.g., from empirical data. Let us illustrate the procedure with specific reference to the tumor growth model recently studied by Zeng and Wang [49]. The governing equation is

$$\begin{cases} \dot{x}(t;\omega) = G(x) + g(x) f_1(t;\omega) + f_2(t;\omega) \\ x(0;\omega) = x_0(\omega) \end{cases} \tag{35}$$

where $x(t;\omega)$ denotes the tumor cell population at time t

$$G(x) \overset{\text{def}}{=} x(1-\theta x) - \beta \frac{x}{x+1}, \quad g(x) \overset{\text{def}}{=} -\frac{x}{x+1}, \tag{36}$$

β is the immune rate, and θ is related to the rate of growth of cytotoxic cells. The random process $f_1(t;\omega)$ represents the strength of the treatment (i.e., the dosage of the medicine in chemotherapy or the intensity of the ray in radiotherapy) while the process $f_2(t;\omega)$ is related to other factors, such as drugs and radiotherapy, that restrain the number of tumor cells. The

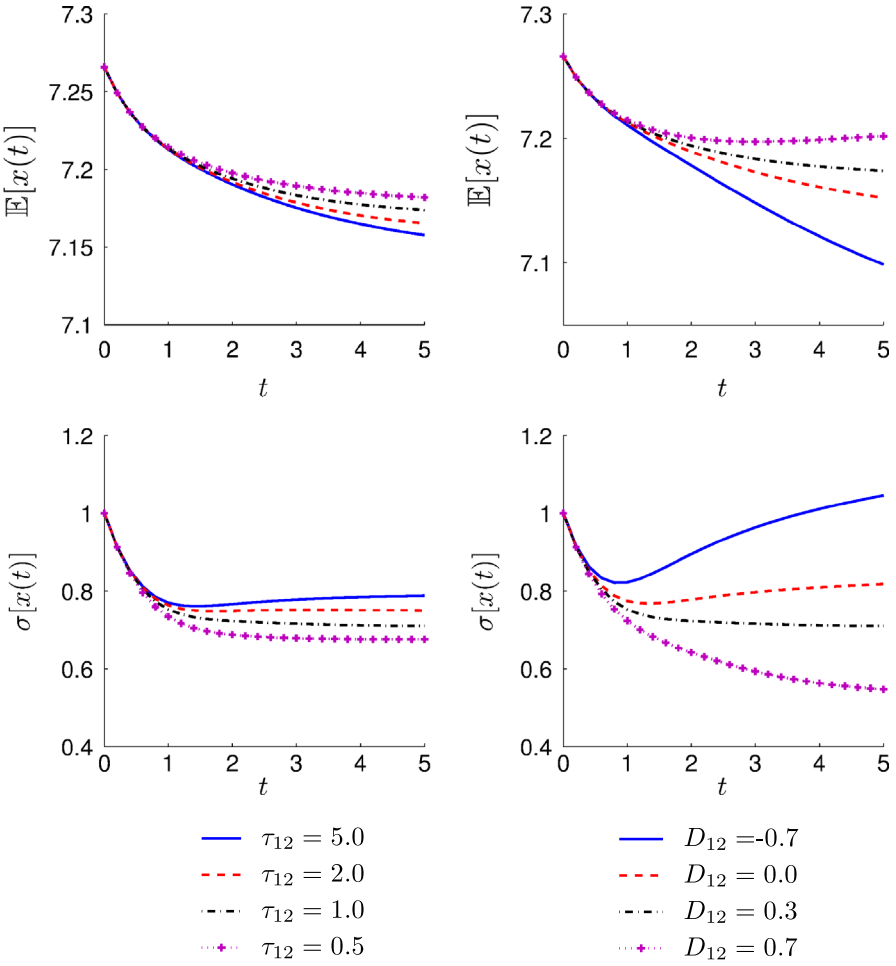

Fig. 12. Mean (first row) and standard deviation (second row) of the tumor population. The covariance kernels of the random processes f_1 and f_2 are assumed to be Gaussian with parameters $\tau_1 = \tau_2 = 0.5$, $D_1 = D_2 = 0.1$, $D_{12} = 0.3$ (left column) and $\tau_1 = \tau_2 = 0.5$, $\tau_{12} = 1$, $D_1 = D_2 = 0.1$ (right column). Note that the statistical properties of tumor population are significantly affected by the cross-covariance structure of the noise.

parameters β, θ and the covariance structure of the random processes f_1 and f_2 are usually estimated by using empirical data. In the present paper, we assume that $f_1(t;\omega)$ and $f_2(t;\omega)$ are cross-correlated Gaussian processes with zero mean and Gaussian correlation functions given in Eq. (3). We also set $\beta = 2.26$ and $\theta = 0.1$. The initial condition $x_0(\omega)$ for the tumor density is assumed to be a standard Gaussian variable with mean $\langle x_0(\omega)\rangle = 7.266$ and unit variance. Such a mean value corresponds to the state of stable tumor in the absence of random noise [49]. We represent the random forcing processes f_1 and f_2 by using both the muKL or mcKL methods. This allows us to solve the stochastic ODE (35) with a high-order probabilistic collocation method [50]. We also employ sparse collocation of level three [51] when the number of random variables in the forcing terms exceeds four. In Fig. 12 we show the mean and the standard deviation of the tumor population $x(t;\omega)$ obtained by using mcKL expansions of random forcing processes with different cross-covariance structure. The dimension of each random process is at most 12 in all cases. When we set $D_{12} = 0.3$, the mean population decays slower with smaller variance for smaller values of τ_{12}. On the other hand, if we set $\tau_{12} = 1$ and change D_{12}, a similar phenomenon happens for larger values of D_{12}. The mean population decays much faster with increasing variance when D_{12} is negative. Similar results are obtained by using mcKL expansion. We conclude that the solution of the tumor cell growth model is significantly affected by the cross-covariance structure of the random input processes f_1 and f_2. Therefore it is of fundamental importance to have available techniques, such as those developed in the present paper, capable of representing effectively the correlation structure of multiple random processes.

5. Summary

In this paper, we proposed two different methods to represent multi-correlated non-stationary stochastic processes. The first method (muKL) is based on the spectral decomposition of a suitable *assembled process* and yields series expansions in terms of an identical set of *uncorrelated* random variables. A similar strategy has been proposed in the context of functional principal component analysis by Ramsay and Silverman [35]. The second method (mcKL) relies on expansions in terms of *correlated* sets of random variables reflecting the cross-covariance structure of the processes. In some sense, muKL can be regarded as a combination of KL expansion and orthogonal polynomial methods [1]. A similar idea was developed independently by Vořechovský [34], but the method is restricted to the case where the auto-covariances are identical. We demonstrated the effectiveness and the computational efficiency of the proposed algorithms through numerical examples involving Gaussian processes with exponential and Gaussian covariances as well as fractional Brownian motion and Brownian bridge processes. We found that muKL usually provides better accuracy and convergence rates but it is computationally more expensive than mcKL. The latter approach yields scalable

algorithms and it can be applied to cases where the sets of random variables in each process are different. We used muKL and mcKL approaches to model and simulate cross-correlated random processes in a stochastic tumor model and found that the response of the system is significantly affected by the cross-correlation structure of the noise. More general applications to systems driven by multiple correlated processes such as those arising in the stochastic modeling of materials and devices can be readily done.

Acknowledgments

This work was supported by OSD-MURI grant FA9550-09-1-0613, by DOE grant DE-SC0009247, and NSF/DMS-1216437.

References

[1] Zhang J, Ellingwood B. Orthogonal series expansions of random processes in reliability analysis. Journal of Engineering Mechanics 1994;120:2660–77.
[2] Li CC, Der-Kiureghian A. Optimal discretization of random processes. Journal of Engineering Mechanics 1993;119:1136–54.
[3] Shinozuka M. Simulation of multivariate and multidimensional random processes. Journal of the Acoustical Society of America 1971;49(1B):357–68.
[4] Shinozuka M, Deodatis G. Simulation of the stochastic process by spectral representation. Applied Mechanics Reviews 1991;44:29–53.
[5] Grigoriu M. On the spectral representation method in simulation. Probabilistic Engineering Mechanics 1993;8:75–90.
[6] Grigoriu M. Evaluation of Karhunen–Lòeve, spectral, and sampling representations for stochastic processes. Journal of Engineering Mechanics 2006;132:179–89.
[7] Dijkerman R, Mazumdar RR. Wavelet representations of stochastic processes and multiresolution stochastic models. IEEE Transactions on Signal Processing 1994;42:1640–52.
[8] Masry E. The wavelet transform of stochastic processes with stationary increments and its application to fractional Brownian motion. IEEE Transactions on Information Theory 2002;39:260–4.
[9] Spanos PD, Tezcan J, Tratskas P. Stochastic processes evolutionary spectrum estimation via harmonic wavelets. Computer Methods in Applied Mechanics and Engineering 2005;194:1367–83.
[10] Ghanem RG, Spanos PD. Stochastic finite elements: a spectral approach. Springer-Verlag; 1998.
[11] Papoulis A. Probability, random variables and stochastic processes. third ed. McGraw-Hill; 1991.
[12] Holmes P, Lumley JL, Berkooz G. Turbulence, coherent structures, dynamical systems and symmetry. Cambridge University Press; 1996.
[13] Chien Y, Fu KS. On the generalized Karhunen–Loève expansion. IEEE Transactions on Information Theory 1967;13:518–20.
[14] Levy A, Rubinstein J. Hilbert-space Karhunen–Loève transform with application to image analysis. Journal of the Optical Society of America A 1999;16:28–35.
[15] Huang SP, Quek ST, Phoon KK. Convergence study of the truncated Karhunen–Loève expansion for simulation of stochastic processes. International Journal for Numerical Methods in Engineering 2001;52:1029–43.
[16] Venturi D. On proper orthogonal decomposition of randomly perturbed fields with applications to flow past a cylinder and natural convection over a horizontal plate. Journal of Fluid Mechanics 2006;559:215–54.
[17] Venturi D. A fully symmetric nonlinear biorthogonal decomposition theory for random fields. Physica D 2011;240(4–5):415–25.
[18] Venturi D, Wan X, Karniadakis GE. Stochastic low-dimensional modelling of a random laminar wake past a circular cylinder. Journal of Fluid Mechanics 2008;606:339–67.
[19] Aubry N, Lima R. Spatiotemporal and statistical symmetries. Journal of Statistical Physics 1995;81(3/4):793–828.
[20] Ramsay JO, Dalzell CJ. Some tools for functional data analysis. Journal of the Royal Statistical Society B 1991;53(3):539–72.
[21] Rice JA, Silverman BW. Estimating the mean and covariance structure nonparametrically when the data are curves. Journal of the Royal Statistical Society B 1991;53(1):233–43.
[22] Yang W, Muller H, Stadtmuller U. Functional singular component analysis. Journal of the Royal Statistical Society B 2011;73(3):303–24.
[23] Hall P, Hosseini-Nasab M. On properties of functional principal components analysis. Journal of the Royal Statistical Society B 2006;68(1):109–26.
[24] Li Y, Kareem A. Simulation of multivariate nonstationary random processes: hybrid DFT and digital filtering approach. Journal of Engineering Mechanics 1997;123:1302–10.
[25] Bolotin VV. Statistical methods in structural mechanics. San Francisco: Holden-Day; 1969.
[26] Shlesinger MF, Swean T. Stochastically excited nonlinear ocean structures. World Scientific; 1998.
[27] Spyrou KJ, Thompson JMT. The nonlinear dynamics of ships. The Royal Society; 2000.
[28] Coyette JP, Meerbergen K. An efficient computational procedure for random vibro-acoustic simulations. Journal of Sound and Vibration 2008;310:448–58.
[29] Torquato S. Random heterogeneous materials: microstructure and macroscopic properties. New York: Springer-Verlag; 2002.
[30] Wittig LE, Sinha AK. Simulation of multicorrelated random processes using the FFT algorithm. Journal of the Acoustical Society of America 1975;58:630–4.
[31] Tipping ME, Bishop CM. Probabilistic principal component analysis. Journal of the Royal Statistical Society B 1999;61:611–22.
[32] Tipping ME, Bishop CM. Mixtures of probabilistic principal component analysis. Neural Computation 1999;11:443–82.
[33] Li WJ, Yeung DY, Zhang Z. Probabilistic relational PCA. Advances in Neural Information Processing Systems 2009;22:1123–31.
[34] Vořechovský M. Simulation of simply cross correlated random fields by series expansion methods. Structural Safety 2008;30:337–63.
[35] Ramsay J, Silverman BW. Functional data analysis (Springer series in statistics). second ed.Springer; 2005.
[36] Xiu D, Karniadakis GE. The Wiener–Askey polynomial chaos for stochastic differential equations. SIAM Journal on Scientific Computing 2002;24(2):619–44.
[37] Foo J, Karniadakis GE. Multi-element probabilistic collocation method in high dimensions. Journal of Computational Physics 2010;229:1536–57.
[38] Yamazaki F, Shinozuka M. Simulation of stochastic fields by statistical preconditioning. Journal of Engineering Mechanics 1990;116(2):268–87.
[39] Deodatis G. Non-stationary stochastic vector processes: seismic ground motion applications. Probabilistic Engineering Mechanics 1996;11:149–68.
[40] Grigoriu M. A class of models for non-stationary Gaussian processes. Probabilistic Engineering Mechanics 2003;18:203–13.
[41] Kato T. Perturbation theory for linear operators. fourth ed. Springer-Verlag; 1995.
[42] Riesz F, Sz-Nagy B. Functional analysis. Dover; 1953.
[43] Lebruna R, Dutfoyb A. Do Rosenblatt and Nataf isoprobabilistic transformations really differ? Probabilistic Engineering Mechanics 2009;24(4):577–84.
[44] Jardak M, Su CH, Karniadakis GE. Spectral polynomial chaos solutions of the stochastic advection equation. Journal of Scientific Computing 2002;17:319–38.
[45] Spanos P, Beer M, Red-Horse J. Karhunen–Loève expansion of stochastic processes with a modified exponential covariance kernel. Journal of Engineering Mechanics 2007;133:773–9.
[46] Schwab C, Todor RA. Karhunen–Loève approximation of random fields by generalized fast multipole methods. Journal of Computational Physics 2006;217(1):100–22.
[47] Yao F, Muller H, Wang JL. Functional data analysis for sparse longitudinal data. Journal of the American Statistical Association 2005;100(470):577–90.
[48] Fiasconaro A, Spagnolo B, Ochab-Marcinek A, Gudowska-Nowak E. Co-occurrence of resonant activation and noise-enhanced stability in a model of cancer growth in the presence of immune response. Physical Review E 2006;74(4):041904 (10pp).
[49] Zeng C, Wang H. Colored noise enhanced stability in a tumor cell growth system under immune response. Journal of Statistical Physics 2010;141:889–908.
[50] Xiu D, Hesthaven J. High-order collocation methods for differential equations with random inputs. SIAM Journal of Scientific Computing 2005;27(3)1118–39.
[51] Novak E, Ritter K. Simple cubature formulas with high polynomial exactness. Constructive Approximation 1999;15:499–522.